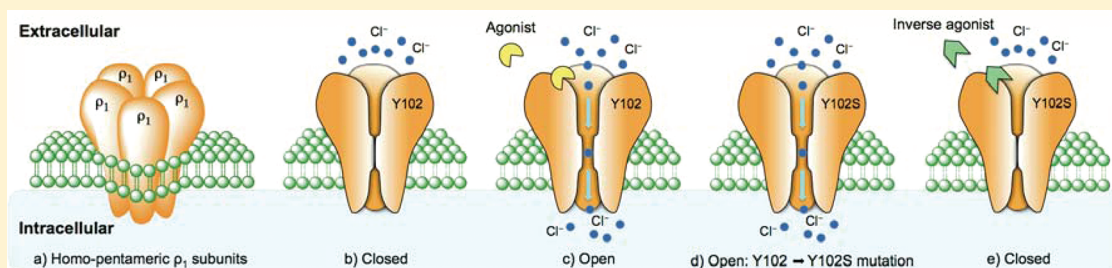


Structurally Diverse GABA Antagonists Interact Differently with Open and Closed Conformational States of the ρ_1 ReceptorIzumi Yamamoto,[†] Jane E. Carland,[‡] Katherine Locock,[‡] Navnath Gavande,[†] Nathan Absalom,[†] Jane R. Hanrahan,[†] Robin D. Allan,[‡] Graham A. R. Johnston,[‡] and Mary Chebib^{*,†}[†]Faculty of Pharmacy and [‡]Department of Pharmacology, The University of Sydney, Sydney, NSW 2006, Australia

S Supporting Information



ABSTRACT: Ligands acting on receptors are considered to induce a conformational change within the ligand-binding site by interacting with specific amino acids. In this study, tyrosine 102 (Y102) located in the GABA binding site of the ρ_1 subunit of the GABA_C receptor was mutated to alanine (ρ_{1Y102A}), serine (ρ_{1Y102S}), and cysteine (ρ_{1Y102C}) to assess the role of this amino acid in the action of 12 known and 2 novel antagonists. Of the mutated receptors, ρ_{1Y102S} was constitutively active, providing an opportunity to assess the activity of antagonists on ρ_1 receptors with a proportion of receptors existing in the open conformational state compared to those existing predominantly in the closed conformational state. It was found that the majority of antagonists studied were able to inhibit the constitutive activity displayed by ρ_{1Y102S} , thus displaying inverse agonist activity. The exception was (\pm)-4-aminocyclopent-1-enecarboxamide ((\pm)-4-ACPAM) (**8**) not exhibiting any inverse agonist activity, but acting explicitly on the closed conformational state of ρ_1 receptors (ρ_1 wild-type, ρ_{1Y102C} and ρ_{1Y102A}). It was also found that the GABA antagonists were more potent at the closed compared to the open conformational states of ρ_1 receptors, suggesting that they may act by stabilizing closed conformational state and thus reducing activation by agonists. Furthermore, of the antagonists tested, Y102 was found to have the greatest influence on the antagonist activity of gabazine (SR-95531 (**13**)) and its analogue (SR-95813 (**14**)). This study contributes to our understanding of the mechanism of inverse agonism. This is important, as such agents are emerging as potential therapeutics.

KEYWORDS: Cys-loop receptor, GABA_C receptors, GABA binding site, gating, conformational change

γ -Aminobutyric acid (GABA) is the major inhibitory neurotransmitter in the mammalian central nervous system (CNS), activating three receptors termed GABA_A , GABA_B , and GABA_C . The GABA_C receptor is found on the retina and at distinct anatomical areas within the CNS, including the superior colliculus,¹ cerebellum,² hippocampus,³ and lateral amygdala,⁴ and has been shown to play an important role in the onset of myopia,⁵ the sleep-waking process,⁶ memory enhancement,⁷ and fear and anxiety disorders.⁴ The design of potent and selective GABA_C receptor antagonists, along with understanding how these agents modulate the receptor, will help characterize these receptors and establish whether GABA_C receptors play a major role in various CNS disorders.^{8,9}

GABA_C receptors belong to the Cys-loop ligand-gated ion channel (LGIC) superfamily.¹⁰ All members of this superfamily require five subunits to form functional receptors. In mammals, GABA_C receptors are composed of three ρ subunits, ρ_1 – ρ_3 , which form homomeric receptors or pseudohomomeric receptors, composed of $\rho_1\rho_2$ or $\rho_2\rho_3$ subunit combina-

tions.^{11–13} The orthosteric binding site of the Cys-loop receptors is located at the interface of two subunits, formed by residues drawn from five discontinuous stretches of amino acids from the N-terminal domain of each subunit. These stretches of residues are referred to as loops A–E. Loops A–C form the principle side of the binding site and loops D and E form the complementary side.¹⁴ GABA_C receptors potentially have five orthosteric or GABA binding sites; GABA binding to these sites induce conformational changes within the receptor that subsequently lead to the opening of the pore, allowing Cl^- ions to pass through.

X-ray crystal structures of related prokaryotic proton-gated ion channels have provided some insights into the structural rearrangement that can occur during receptor gating.¹⁵ ELIC (*Erwinia chrysanthemum* ligand-gated ion channel) represents an

Received: November 30, 2011

Accepted: January 13, 2012

Published: January 13, 2012

inactive receptor conformation and GLIC (*Gloeobacter violaceus* ligand-gated ion channels) represents a desensitized receptor conformation.^{16,17} Despite a lack of mammalian crystal structures, there is strong evidence that structural changes occur within the orthosteric binding site upon activation of the receptor by GABA¹⁸ and that the binding site is constricted in the open conformation.¹⁹

Tyrosine at position 102 (Y102) is located on loop D of the ρ_1 subunit within the GABA binding site. This residue has been proposed to be associated with agonist binding and channel gating.²⁰ Recently, this residue was demonstrated not to form a cation- π interaction with GABA²¹ and in an alternative homology model of the ρ_1 GABA binding site implicates that this residue does not directly bind GABA.²² Mutation of Y102 to serine (ρ_{1Y102S}) in the ρ_1 subunit shifts the equilibrium of the receptor toward the open conformation, producing a constitutively active form of the receptor.²⁰ The competitive antagonist 3-aminopropyl-methyl-phosphinic acid (3-APMPA) inhibits the spontaneous current of ρ_{1Y102S} receptors in a concentration-dependent manner,²⁰ demonstrating that 3-APMPA acts as an inverse agonist, inducing a conformational change which shifts the equilibrium of the receptor toward the closed conformation.

In this study, the role of Y102 in antagonist activity was assessed. Y102 was mutated to serine (ρ_{1Y102S}), cysteine (ρ_{1Y102C}), and alanine (ρ_{1Y102A}), and the resulting mutant receptors represent channels with a proportion in the open conformational state (ρ_{1Y102S}) and almost entirely in the closed conformational state (ρ_{1Y102C} , ρ_{1Y102A}) of the channel. Twelve known antagonists (1–7 and 9–13) and two novel antagonists (8 and 14) were evaluated on ρ_1 wild-type and mutant receptors to investigate if antagonist activity was altered with receptor conformation.

RESULTS AND DISCUSSION

The mechanism by which an agonist binds and subsequently opens the channel of Cys-loop receptors is complex and involves many structural changes throughout the receptor, including changes within the orthosteric binding site. Ligands, for example, 3-APMPA (2), have different affinities for the open or closed conformational states of the receptor, as the conformation of the binding site differs between the two conformational states.²⁰ Constitutively active receptors, such as the ρ_{1Y102S} receptor, provide an opportunity to assess the activity of antagonists on receptors in equilibrium between the open or closed conformational states of the receptor.

ρ_{1Y102S} Receptors Are Constitutively Active. Consistent with previous studies,²⁰ the EC_{50} values for GABA increased by 21-, 233- and 196-fold when ρ_1 Y102 was mutated to cysteine, serine, and alanine, respectively (Figure 1, Table 1). This change in GABA sensitivity suggests that mutation of Y102 on the ρ_1 subunit results in a change in GABA affinity or altered receptor gating. Of the three mutant receptors evaluated, ρ_{1Y102S} receptors were constitutively active. When clamped at -60 mV, the holding current for cells expressing ρ_{1Y102S} (-200.3 ± 20.1 nA, $n = 11$) was greater than that in cells expressing ρ_1 wild-type (-15.2 ± 4.0 nA, $n = 11$), ρ_{1Y102A} (-0.2 ± 1.7 nA, $n = 11$), and ρ_{1Y102C} (-5.6 ± 4.1 nA, $n = 11$) mutant receptors. This suggests that while ρ_{1Y102S} receptors exist in equilibrium between the open and closed conformational states, while ρ_1 wild-type, ρ_{1Y102A} , and ρ_{1Y102C} receptors predominantly prefer the closed conformational state.

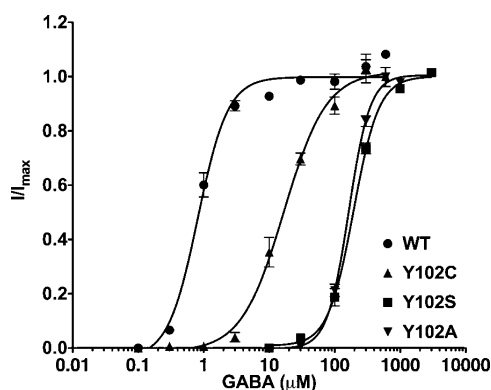


Figure 1. GABA concentration response curves for human ρ_1 wild-type (WT) receptors and ρ_{1Y102C} , ρ_{1Y102S} and ρ_{1Y102A} receptors expressed in *Xenopus* oocytes. Each data point represents the mean \pm SEM ($n = 3-4$). All data are normalized with I_{max} , which refers to their maximum current. EC_{50} values are listed in Table 1.

Table 1. EC_{50} Values for GABA at ρ_1 Wild-Type and Y102 Mutant Receptors^a

ρ_1 Y102 mutation	EC_{50} (μ M)
WT	0.8 ± 0.1
Y102C	17.6 ± 1.2
Y102S	193.7 ± 9.7
Y102A	163.1 ± 2.0

^aAll data are the means \pm SEMs ($n = 3-4$ oocytes).

(\pm)-4-ACPA (8) and SR-95813 (14) Are Potent Antagonists at ρ_1 Receptors. In this study, a total of 12 known and 2 novel agents were evaluated at ρ_1 receptors. TPMPA (1), 3-APMPA (2), SGS-742/CGP-36742 (3), (\pm)-*cis*-3-ACPBPA (4), (\pm)-3-*trans*-ACPBPA (5), S-4-ACBP-PA (6), (+)-S-4-ACPCA (7), THIP (9), DAVA (10), 4-GBA (11), ZAPA (12), and SR-93351/Gabazine (13) have been shown previously to act as competitive antagonists at ρ_1 wild-type receptors, indicating that they bind to the GABA binding site. The activities of two novel ligands, (\pm)-4-ACPA (8) and SR-95813 (14), were characterized at ρ_1 wild-type receptors recombinantly expressed in *Xenopus* oocytes. These novel compounds are interesting in that they do not possess an acid moiety (carboxylic or phosphinic acid), a feature common to all ligands that bind to the GABA binding site. Instead of the usual acid moiety, (\pm)-4-ACPA (8) has an amide group, while SR-95813 (14) has a nitrile group. To our surprise, these compounds were found to be potent ρ_1 receptor competitive antagonists. Figure 2A demonstrates that (\pm)-4-ACPA (8) inhibits the EC_{50} of GABA (1 μ M) in a concentration-dependent manner (Figure 2A, $IC_{50} = 9.6 \pm 0.9$ μ M, $n = 4$). Schild plot analysis demonstrates that in the presence of increasing concentrations of (\pm)-4-ACPA (8) (30, 100, and 300 μ M; $n = 3-4$ oocytes per antagonist concentration), the concentration response curve for GABA is shifted to the right in a parallel manner (Figure 2B, $K_B = 30.3 \pm 3.1$ μ M, slope did not differ from 1, see Figure 2 Supporting Information), indicating that (\pm)-4-ACPA (8) is a competitive antagonist at ρ_1 wild-type receptors.

Similarly, SR-95813 (14) inhibits the response produced by GABA (1 μ M) in a concentration-dependent manner (Figure 2C, $IC_{50} = 8.0 \pm 0.8$ μ M, $n = 4$). Schild plot analysis shows that in the presence of increasing concentrations of SR-95813 (14) (30, 100 and 300 μ M; $n = 3-4$ oocytes per antagonist

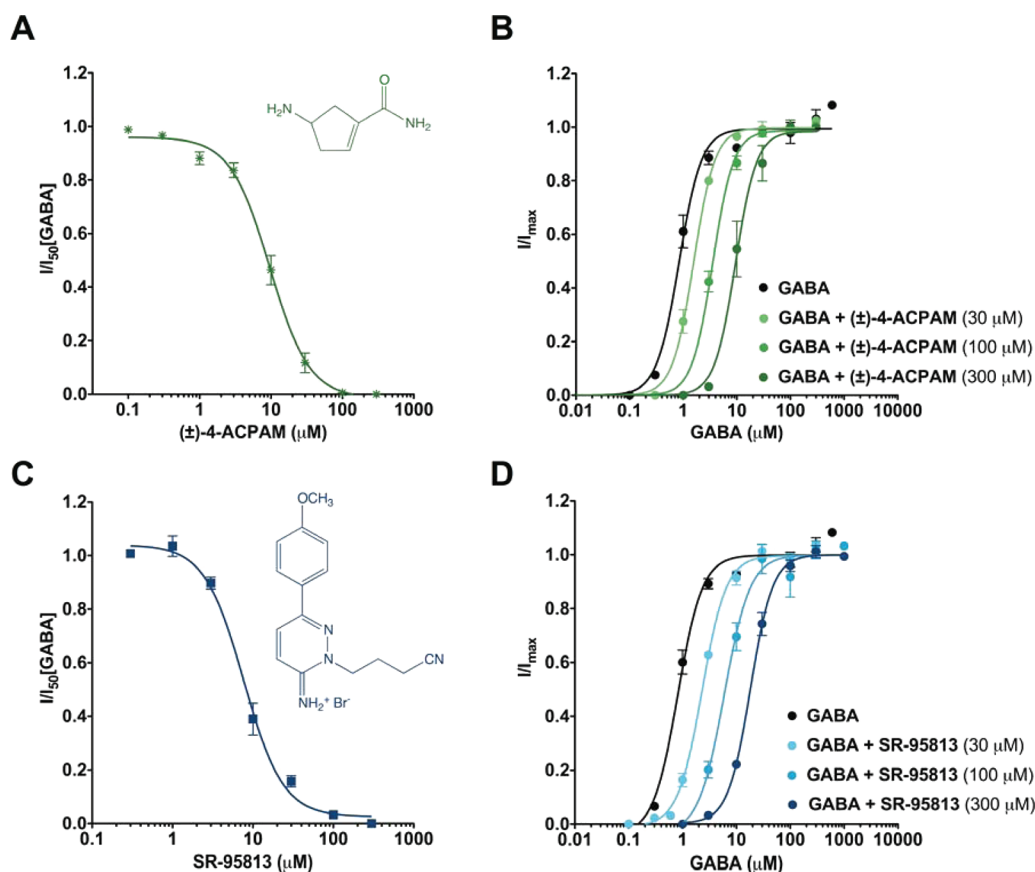


Figure 2. Pharmacology of (±)-4-ACPA (8) and SR-95813 (14) at human ρ_1 wild-type receptors expressed in *Xenopus* oocytes. (A) Inhibitory concentration response curve for (±)-4-ACPA (8) against GABA (1 μ M) at ρ_1 receptors. Each data point represents the mean \pm SEM ($n = 3$ –4). (B) Concentration response curves of GABA alone (black dot, $n = 3$) and in the presence of (±)-4-ACPA (8) at 30 (light green dot, $n = 3$), 100 (green dot, $n = 4$), and 300 μ M (dark green dot, $n = 3$). Each data point represents the mean \pm SEM ($n = 4$). All data are normalized with I_{\max} , which refers to their maximum current. (C) Inhibitory concentration response curve for SR-95813 (14) against GABA (1 μ M) at ρ_1 receptors. Each data point represents the mean \pm SEM ($n = 4$). (D) Concentration response curves of GABA alone (black dot, $n = 4$) and in the presence of SR-95813 (14) at 30 (light blue dot, $n = 3$), 100 (blue dot, $n = 4$), and 300 μ M (dark blue dot, $n = 3$). Each data point represents the mean \pm SEM ($n = 3$ –4). All data are normalized with I_{\max} , which refers to their maximum current.

concentration), the GABA concentration response curve is shifted to the right in a parallel manner (Figure 2D, $K_B = 12.4 \pm 0.4 \mu$ M, slope did not differ from 1, see Figure 2 in the Supporting Information), indicating that SR-95813 (14) blocks ρ_1 wild-type receptors in a competitive manner.

Mutagenesis studies of the ρ_1 receptor identified arginine 104 (R104) as important for GABA binding, and this residue is thought to interact via a salt bridge with the carboxylate group of GABA.²³ Homology models of the ρ_1 receptor support this observation.²² As (±)-4-ACPA (8) and SR-95813 (14) do not possess a carboxylate group, it would be interesting to evaluate R104 in the binding of these ligands.

Assessing the Activity of Antagonists at a Proportion of Receptors in the Open Conformational State. The activities of 14 GABA antagonists (1–14) were evaluated using the constitutively active ρ_{1Y102S} receptors. Antagonists were tested at 100 and 300 μ M in the absence of GABA. The percentage inhibition of the spontaneous current was measured and normalized to the initial resting current for each cell. All antagonists tested inhibited the spontaneous current of ρ_{1Y102S} receptors to a various extent when evaluated at 300 μ M, with the exception of (±)-4-ACPA (8). (±)-4-ACPA (8), at either 100 or 300 μ M, failed to inhibit the spontaneous current at these receptors (Figure 3B).

Of the compounds tested, SGS-742 (3), S-4-ACPCA (7), (±)-4-ACPA (8) and DAVA (10) were the weakest at inhibiting (0–9%) the constitutive current produced by ρ_{1Y102S} receptors. The remaining antagonists inhibited the current by 10–87% (Table 2). 3-APMPA (2) was the most effective inhibitor of the constitutive current, while TPMPA (1), (±)-*cis*-3-ACPBPA (4), 4-GABA (11), SR-95331 (13), and SR-95813 (14) displayed moderate inhibition of the constitutive current.

To explore the relative activity of antagonists on the open conformational state of the ρ_1 receptor, we focused on five structurally different GABA antagonists, TPMPA (1), (±)-*cis*-3-ACPBPA (4), (±)-4-ACPA (8), 4-GABA (11), SR-95331 (13), and SR-95813 (14) (Table 2). Application of the competitive antagonist, TPMPA (1), to ρ_{1Y102S} receptors inhibited the spontaneous current in a concentration-dependent manner (Figure 3A). This indicates that TPMPA shifts the equilibrium of ρ_{1Y102S} receptors from the open to the closed conformational state, thus acting as an inverse agonist (Table 2). However, TPMPA is weak exhibiting a 600-fold decrease in potency.

Figure 3C shows the concentration response curves for TPMPA (1), (±)-*cis*-3-ACPBPA (4), (±)-4-ACPA (8), 4-GABA (11), SR-95331 (13), and SR-95813 (14) inhibiting the spontaneous current of ρ_{1Y102S} receptors. The affinities of the

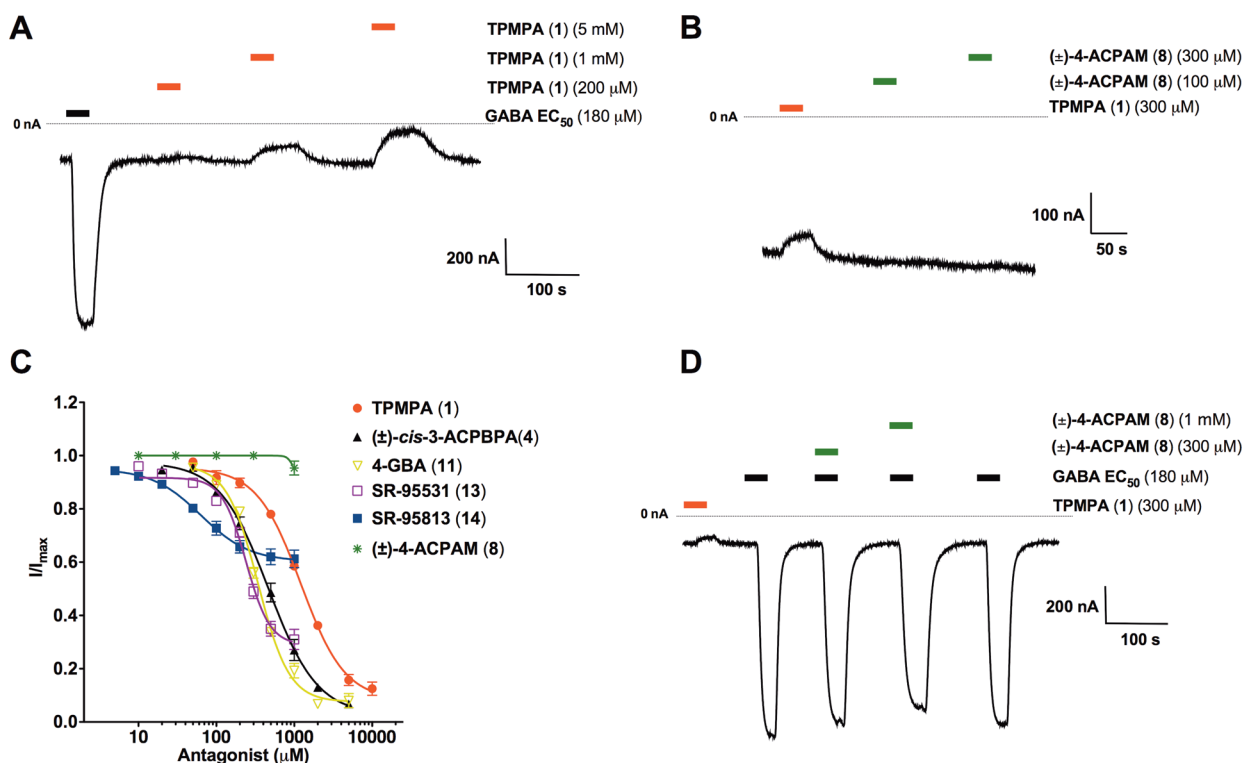


Figure 3. Effect of GABA antagonists at GABA ρ_{1Y102S} receptor spontaneous currents. (A) A sample current traces showing inverse agonist effects of TPMPA (1) at GABA ρ_{1Y102S} receptors expressed in *Xenopus* oocytes. GABA EC_{50} (180 μ M) activates the receptor (black bar), allowing influx of Cl^- ions. Application of TPMPA (1) (200 μ M, 1 mM and 5 mM) alone inhibited the resting conductance in a concentration dependent manner (red bar). (B) A sample current trace showing the effect of (±)-4-ACPA (8) at GABA ρ_{1Y102S} receptor spontaneous current. (±)-4-ACPA (8) did not exhibit inverse agonist effects at 100 μ M and 300 μ M (green bar). (C) Inhibitory concentration–response curves for TPMPA (1) (red), SR-95531 (13) (purple), SR-95813 (14) (blue), (±)-cis-3-ACBPBA (4) (black), and 4-GBA (11) (yellow) on GABA ρ_{1Y102S} receptors expressed in *Xenopus* oocytes. All data are normalized with I_{max} , which refers to the initial resting conductance. Each data point represents the mean \pm SEM ($n = 3-5$). (D) A sample current trace showing weak inhibitions of GABA EC_{50} (180 μ M) (black bar) by (±)-4-ACPA (8) (300 μ M and 1 mM) (green bar) at GABA ρ_{1Y102S} receptors.

compounds against the spontaneous current were lower compared to the ρ_1 wild-type (Tables 2 and 3). The order of potency of the compounds at ρ_{1Y102S} receptors was SR-95813 (14) > SR-95531 (13) > (±)-cis-3-ACBPBA (4) > 4-GBA (11) > TPMPA (1) (Table 3). (±)-4-ACPA (8) had a very small effect on the constitutive activity of ρ_{1Y102S} receptors even at the 1 mM concentration (Figure 3C) and failed to significantly inhibit GABA (EC_{50} ; 180 μ M) at this mutant receptor (Figure 3D).

Interestingly, both SR-95531 (13) and SR-95813 (14) could not completely block the spontaneous current of ρ_{1Y102S} receptors (Figure 3C), indicating they may act as partial inverse agonists at the mutant receptor. Furthermore, in the presence of GABA, both SR-95531 (13) and SR-95813 (14) inhibited GABA with IC_{50} values approximately 2-fold weaker than the EC_{50} value that inhibits the constitutive activity (Table 3 and 4, Figure 4), suggesting the binding affinity of these compounds are similar in the presence or absence of GABA at ρ_{1Y102S} receptors.

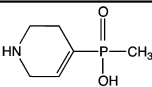
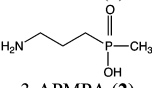
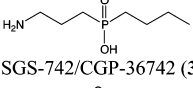
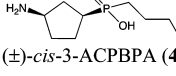
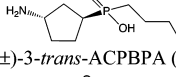
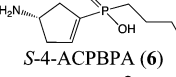
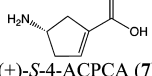
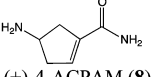
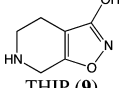
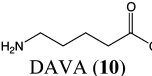
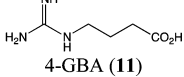
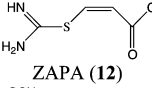
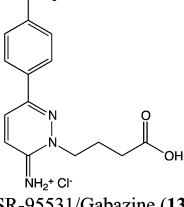
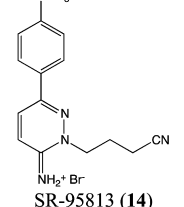
Assessing the Activity of Antagonists at Receptors in the Closed Conformation State. The activities of the five antagonists were examined at ρ_{1Y102C} and ρ_{1Y102A} receptors (Table 4, Figure 5). In contrast to ρ_{1Y102S} receptors, ρ_{1Y102C} and ρ_{1Y102A} receptors were not constitutively active, thus existing predominantly in the closed conformational state. Interestingly, (±)-4-ACPA (8) at a concentration of 300 μ M regained some of its antagonist activity for the ρ_{1Y102C} and ρ_{1Y102A} mutant

receptors (Table 4). At ρ_{1Y102C} receptors, (±)-4-ACPA (8) displayed a 25-fold increase in IC_{50} compared to ρ_1 wild-type (At ρ_1 wild-type; $IC_{50} = 9.6 \pm 0.9 \mu$ M; at ρ_{1Y102C} ; $IC_{50} = 241.8 \pm 17.2 \mu$ M). As (±)-4-ACPA (8) did not inhibit the constitutive activity of ρ_{1Y102S} mutant receptors, nor did it inhibit GABA (Figure 3B and D) or the inverse agonist effects of SR-95531 (13) (see Figure 3 in the Supporting Information) at this receptor, we can infer that either tyrosine is crucial for the binding of (±)-4-ACPA (8) or that (±)-4-ACPA (8) acts at receptors existing predominantly in the closed over the open conformational state.

At ρ_{1Y102C} receptors, the IC_{50} values for TPMPA (1), (±)-cis-3-ACBPBA (4) and 4-GBA (11) were also increased by 200-, 22- and 25-fold, respectively, compared to ρ_1 wild-type receptors (Table 4). As the cysteine and alanine mutations did not affect potency of the antagonists to the same extent as the serine mutation, indicating that these compounds have the ability to preferentially bind to the closed conformational state of the receptor. A similar phenomenon is observed with tetracaine at nicotinic acetylcholine (nACh) receptors.²⁴ Tetracaine has a 100-fold higher affinity for the close conformation compared the desensitized conformation of the *Torpedo* nACh receptor, implicating tetracaine is a closed conformation channel blocker.

In contrast to what was observed at ρ_{1Y102S} receptors, the inhibitory activity of SR-95531 (13) and its analogue SR-95813 (14) was significantly reduced at both ρ_{1Y102C} and ρ_{1Y102A}

Table 2. Effects of Structurally Diverse Antagonists on Recombinant ρ_1 Wild-Type and ρ_{1Y102S} Receptors^a

Compound	Antagonist activity on human ρ_1 wild-type receptors	% inhibition of spontaneous current on ρ_{1Y102S} receptors ^a	
		100 μ M	300 μ M
 TPMPA (1)	$IC_{50} = 2.22 \mu M^b$	8.7 ± 0.3	22.3 ± 2.7
 3-APMPA (2)	$IC_{50} = 0.75 \mu M^c$	47.9 ± 4.7	87.6 ± 6.7
 SGS-742/CGP-36742 (3)	$IC_{50} = 62.5 \mu M^c$	1.4 ± 0.5	4.7 ± 0.3
 (±)-cis-3-ACBPBA (4)	$IC_{50} = 5.06 \mu M^d$	13.8 ± 0.7	33.7 ± 0.4
 (±)-3-trans-ACBPBA (5)	$IC_{50} = 72.58 \mu M^d$	NA	6.6 ± 1.6
 S-4-ACBPBA (6)	$IC_{50} = 4.97 \mu M^e$	5.7 ± 0.6	17.5 ± 0.9
 (+)-S-4-ACPCA (7)	$K_i = 6.0 \mu M^f$	0.3 ± 0.2	2.0 ± 0.6
 (±)-4-ACPAM (8)	$IC_{50} = 9.6 \pm 0.9 \mu M$ $K_B = 30.3 \pm 3.1 \mu M$	NA	NA
 THIP (9)	$IC_{50} = 10 \mu M^g$	1.3 ± 0.7	10.7 ± 0.3
 DAVA (10)	$K_B = 20 \mu M^h$	2.2 ± 0.5	5.5 ± 0.2
 4-GBA (11)	$IC_{50} = 18.75 \mu M^i$	13.5 ± 1.3	37.8 ± 3.1
 ZAPA (12)	$IC_{50} = 11 \mu M^g$	3.2 ± 1.1	9.9 ± 0.8
 SR-95531/Gabazine (13)	$IC_{50} = 60.7 \pm 12.6 \mu M^j$ $K_B = 51.2 \pm 2.9 \mu M^k$	16.4 ± 1.3	28.8 ± 5.9
 SR-95813 (14)	$IC_{50} = 8.0 \pm 0.8 \mu M$ $K_B = 12.4 \pm 0.4 \mu M$	25.0 ± 2.0	33.3 ± 1.7

^aPercentage inhibitions of ρ_{1Y102S} receptor spontaneous currents by compounds (100 and 300 μ M), which were normalized by initial resting conductance. All data are the mean \pm SEMs ($n = 3-12$ oocytes). ^bData from ref 8. ^cData from ref 36. ^dData from ref 37. ^eData from ref 29. ^fData

Table 2. continued

from ref 38. ^gData from ref 39. ^hData from ref 13. ⁱData from ref 31. ^jSee Figure 1 in Supporting Information. ^kSee Figure 2 in Supporting Information. NA stands for not active at the concentration.

Table 3. EC₅₀ Values of TPMPA (1), SR-95531 (13), SR-95813, ¹⁴ (±)-cis-3-ACBPBA (4), and 4-GBA (11) on GABA ρ_{1Y102S} Receptors^a

compd	EC ₅₀ (μ M) ^b
TPMPA (1)	1234.3 \pm 57.7
SR-95531 (13)	312.9 \pm 15.1
SR-95813 (14)	64.3 \pm 2.8
(±)-cis-3-ACBPBA (4)	488.3 \pm 60.5
4-GBA (11)	568.7 \pm 25.3

^aData are the means \pm SEMs (n = 4–5 oocytes). ^bConcentration which inhibits 50% of the maximum spontaneous current of ρ_{1Y102S} receptor.

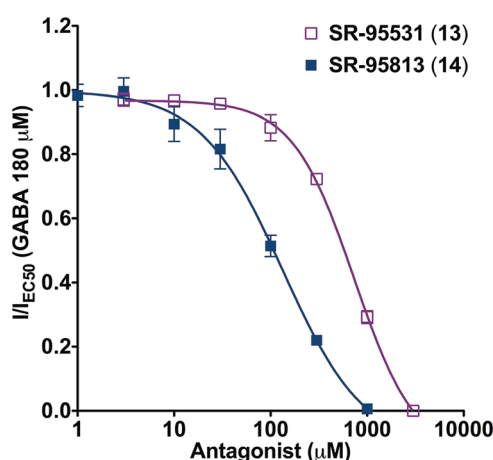


Figure 4. Inhibitory concentration–response curves for SR-95531 (13) and SR-95813 (14) at GABA ρ_{1Y102S} receptors expressed in *Xenopus* oocytes. Each data point represents the mean \pm SEM (n = 3–5). All antagonists were tested in the presence of GABA EC₅₀ (180 μ M). All data are normalized with $I_{EC50}[GABA]$.

receptors. SR-95531 (13) (300 μ M) inhibited only 7.5% of the current elicited by GABA EC₅₀ (20 μ M) at ρ_{1Y102C} receptors and was inactive at ρ_{1Y102A} receptors (Figure 6, Table 4). Furthermore, SR-95813 (14) (300 μ M) did not inhibit the current elicited by GABA EC₅₀ (20 μ M) at both ρ_{1Y102C} and

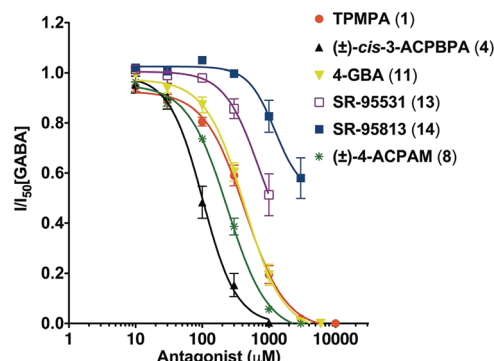


Figure 5. Inhibitory concentration–response curves for TPMPA (1), (±)-cis-3-ACBPBA (4), 4-GBA (11), SR-95531 (13), SR-95813 (14), and (±)-4-ACPAM (8) at GABA ρ_{1Y102C} receptors expressed in *Xenopus* oocytes. Each data point represents the mean \pm SEM (n = 3–5). All antagonists were tested in the presence of GABA EC₅₀ (20 μ M). All data are normalized with $I_{EC50}[GABA]$.

ρ_{1Y102A} receptors (Figure 6, Table 4). Thus, the order of potency of the compounds tested at ρ_{1Y102C} receptors was (±)-cis-3-ACBPBA (4) > (±)-4-ACPAM (8) > 4-GBA (11) \approx TPMPA (1) \gg SR-95531 (13) \approx SR-95813 (14). As SR-95531 (13) and its analogue SR-95813 (14) are more potent on ρ_{1Y102S} than ρ_{1Y102C} receptors, may indicate that the compounds are more likely to bind to the open over the closed conformational state of the receptor. While we cannot rule out the possibility of direct interaction between the introduced residues and the antagonists tested, there is no clear structure activity relationship to suggest that either possibility may be the case.

Previous studies have shown that mutating Y102 of the ρ_1 subunit to phenylalanine alters the effect of SR-95531 (13)²⁵ and that the mutation of the homologous residue in the GABA_A receptor α_1 -subunit (phenylalanine at position 64) to cysteine dramatically changes the affinity of SR-95531.²⁶ The data presented in this study using SR-95531 (13), SR-95813 (14), (±)-cis-3-ACBPBA (4), (±)-4-ACPAM (8), 4-GBA (11), and TPMPA (1) provides further support that Y102 plays a key role

Table 4. Effect of ρ_1 Y102 Mutations on the Activity of Selected Antagonists in the Presence of GABA EC₅₀^a

compd	% inhibition of GABA EC ₅₀ by selected compounds				
	WT	Y102S	Y102C	Y102A	
	300 μ M ^b	300 μ M ^b	300 μ M ^b	IC ₅₀ (μ M) ^c	300 μ M ^b
TPMPA (1)	100.0 \pm 0.0%	13.0 \pm 1.5%	49.7 \pm 5.5%	447.2 \pm 50.9	25.1 \pm 4.4%
(±)-cis-3-ACBPBA (4)	100.0 \pm 0.0%	22.5 \pm 2.4%	90.8 \pm 2.6%	110.7 \pm 22.6	74.1 \pm 11.5%
(±)-4-ACPAM (8)	100.0 \pm 0.0%	inactive at 300 μ M	68.5 \pm 2.1%	241.8 \pm 17.2	21.0 \pm 1.0%
4-GBA (11)	98.9 \pm 0.6%	9.8 \pm 2.8%	50.6 \pm 7.1%	460.1 \pm 58.1	47.9 \pm 7.1%
SR-95531 (13)	96.0 \pm 0.9%	775.7 \pm 54.9 μ M ^d	7.5 \pm 4.1%	50.7 \pm 6.4% ^e	inactive at 300 μ M
SR-95813 (14)	98.8 \pm 1.2%	135.2 \pm 16.0 μ M ^d	inactive at 300 μ M	17.3 \pm 6.4% ^e	inactive at 300 μ M

^aAll data are the mean \pm SEM (n = 3 oocytes). ^bData are percentage inhibition of the current produced by EC₅₀ (submaximal concentration) of GABA by selected compounds (300 μ M). EC₅₀ (submaximal concentration) values for GABA at ρ_1 wild-type, ρ_{1Y102S} , ρ_{1Y102C} , and ρ_{1Y102A} mutant receptors are 1, 180, 20, and 200 μ M, respectively. All data are the means \pm SEMs (n = 3–6 oocytes). ^cCompound concentration of which inhibits EC₅₀ of GABA (20 μ M) on ρ_{1Y102C} receptors. ^dCompound concentration of which inhibits EC₅₀ of GABA (180 μ M) at ρ_{1Y102S} receptors. ^eData are percentage inhibition of the current produced by EC₅₀ of GABA (20 μ M) by SR-95531 (13) and SR-95813 (14) (1 mM).

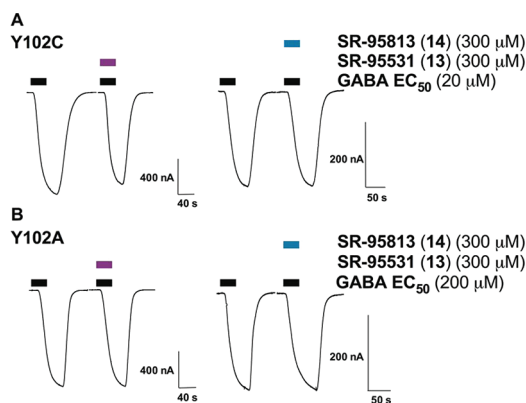


Figure 6. Sample current trace showing the effect of SR-95531 (13) and SR-95813 (14) at GABA ρ_{Y102C} and ρ_{Y102A} receptors in *Xenopus* oocytes. (A) The current produced by GABA (20 μ M) (black bar) was inhibited by 7.5% in the presence of SR-95531 (13) (300 μ M, purple bar), and SR-95813 (14) (300 μ M, dark blue) did not inhibit the current produced by GABA (20 μ M, black bar) at ρ_{Y102C} mutated receptors. (B) SR-95531 (13) (300 μ M, purple bar), and SR-95813 (14) (300 μ M, dark blue) did not inhibit the current produced by GABA (200 μ M, black bar) at ρ_{Y102A} mutated receptor.

in binding/gating. However, the activity of SR-95531 (13) and its analogue SR-95813 (14) is not dramatically changed when ρ_{Y102} is mutated to serine. This indicates that, at least with the gabazine analogues, π - π interactions are not the main interactions affecting the activity of these compounds at ρ_1 receptors, despite an improved affinity of SR-95531 (13) when Y102 is mutated to phenylalanine.²⁵ This supports the homology model which infers that Y102 does not directly interact with GABA²² and is most likely a residue involved in channel gating. In support of this conclusion, the partial agonist imidazole-4-acetic acid (I4AA) activated the ρ_{Y102C} mutant receptor with high efficacy and lower potency compared to ρ_1 wild-type,²⁰ consistent with Y102 being a residue involved in gating.

CONCLUSION

In conclusion, the affinity of ρ_1 receptor antagonists is dependent on the receptor conformation as a result of the introduced mutations. In this study we investigated the potencies of a range of antagonists at ρ_1 wild-type, ρ_{Y102S} , ρ_{Y102C} , and ρ_{Y102A} mutant receptors. It was found that the acid moiety that is a common feature of most ρ_1 antagonists was not found to be critical for antagonist activity, as demonstrated with (\pm)-4-ACPA (8) and SR-95813 (14). We also confirmed that Y102 plays important role in the potency of (\pm)-4-ACPA (8), SR-95531 (13) and SR-95813 (14). In addition, (\pm)-4-ACPA (8) is more potent for closed conformational state of the ρ_1 receptor, while SR-95531 (13) and its analogue SR-95813 (14) are more potent where there are receptors in the open conformational state.

METHODS

Chemicals. TPMPA [(1,2,5,6-tetrahydropyridin-4-yl)-methylphosphinic acid],²⁷ (\pm)-*cis*-3-ACBPA [(\pm)-*cis*-(3-aminocyclopentyl)butylphosphinic acid],²⁸ (\pm)-*trans*-3-ACBPA [(\pm)-*trans*-(3-aminocyclopentyl)butylphosphinic acid],²⁸ (*S*)-4-ACBPA [(*S*)-4-amino-1-cyclopent-1-enyl(butyl)phosphinic acid],²⁹ (+)-4-ACPA [(+)-4-aminocyclopent-1-ene-1-carboxylic acid],³⁰ 4-GABA (4-guanidinobutanoic acid),³¹ ZAPA [(*Z*)-3-[(aminoiminomethyl)thio]

prop-2-enoic acid],³² SR-95531 (gabazine),³³ and SR-95813³³ were synthesized according to our previously published methods.^{27–33}

GABA (γ -aminobutyric acid), THIP (4,5,6,7-tetrahydroisoxazolo-[5,4-*c*]pyridin-3-ol), and DAVA (5-aminovaleric acid) were purchased from Sigma-Aldrich Chemical Co. (St Louis, MO). 3-APMPA (3-aminopropyl(methyl)phosphinic acid) was purchased from Tocris Bioscience (Bristol, U.K.). CGP-36742 or SGS-742 (3-aminopropyl-*n*-butylphosphinic acid) was a gift from Dr. Wolfgang Froestl (formerly Novartis, Switzerland).

Synthetic Procedure and Characterization Data for (\pm)-4-ACPA (8) ((\pm)-4-Aminocyclopent-1-enecarboxamide). Methyl 4-*tert*-butoxycarbonylamino-cyclopent-1-enecarboxylate³⁴ (2.90 g, 12 mmol) was added to an aqueous solution of 0.5 M sodium hydroxide (80 mL) and tetrahydrofuran (40 mL) and allowed to stir overnight at room temperature. Excess tetrahydrofuran was removed from this solution under reduced pressure followed by extraction with dichloromethane (60 mL). The remaining aqueous fraction was acidified to pH 3 with 10% aqueous citric acid in the presence of dichloromethane (180 mL). The combined organic phases were dried over magnesium sulfate and evaporated to give 4-*tert*-butoxycarbonylamino-cyclopent-1-enecarboxylic acid (2.59 g, 95% yield). R_f = 0.35 (4:1 ethyl acetate/petroleum ether). ¹H NMR (300 MHz, CDCl₃): δ 6.86 (1H, s, HC=), 4.75 (1H, br s, NH), 4.39 (1H, bs, C(4)H), 2.97 (2H, bt, J = 9 Hz, C(3)H and C(5)H), 2.49–2.39 (2H, m, C(3)H and C(5)H), 1.45 (9H, s, Boc). ¹³C NMR (300 MHz, CDCl₃): δ 168.96 (C=O), 143.94 (=C), 134.27 (HC=), 79.80 (C(CH₃)₃), 50.40 (CHNHBoc), 41.57 (cyclopentene CH₂), 39.03 (cyclopentene CH₂), 28.60 (C(CH₃)₃). CI-MS m/z 154 (52%, MH⁺-C₄H₈O), 126 (100, MH⁺-Boc), 93 (14, MH⁺-Boc-H₂O), 82 (45, MH⁺-Boc-CO₂).

Triethylamine (304 mg, 3 mmol) was added to a solution of 4-*tert*-butoxycarbonylamino-cyclopent-1-enecarboxylic acid (7, 341 mg, 1.5 mmol) in tetrahydrofuran (30 mL) at 0 °C. *iso*-Butylchloroformate (338 mg, 2.5 mmol) was added dropwise, and the solution left to stir for 15 min. Gaseous ammonia was bubbled through the solution for 20 min and the reaction left to stir at 0 °C for a further 2 h. The reaction was concentrated in vacuo, diluted with ethyl acetate (30 mL), and washed with aqueous sodium hydroxide (1 M, 10 mL), saturated citric acid (10 mL), and brine (10 mL). The organic fraction was dried over sodium sulfate and solvent was removed under reduced pressure. The product was isolated using flash chromatography, eluting with ethyl acetate/dichloromethane (10:1) to give *tert*-butyl 3-carbamoylcyclopent-3-enylcarbamate (315 mg, 92% yield). R_f = 0.47 (ethyl acetate). ¹H NMR (300 MHz, CDCl₃): δ 6.52 (1H, s, HC=), 5.72–5.18 (2H, br d, NH₂), 4.85–4.64 (1H, m, C(4)H), 4.40 (1H, br s, NHBoc), 3.04–2.84 (2H, m, C(3)H and C(5)H), 2.52–2.33 (2H, m, C(3)H and C(5)H), 1.45 (9H, s, Boc). ¹³C NMR (300 MHz, CDCl₃): δ 166.76 ((C=O)NH₂), 155.57 ((C=O)Ot-Bu), 137.01 (HC=), 136.91 (=C), 79.80 (C(CH₃)₃), 50.65 (CHNHBoc), 41.14 (cyclopentene CH₂), 39.64 (cyclopentene CH₂), 28.60 (C(CH₃)₃). *tert*-Butyl 3-carbamoylcyclopent-3-enylcarbamate (315 mg, 1.39 mmol) was dissolved in a saturated solution of hydrochloric acid in ethyl acetate and the resulting solution allowed to stir for 4 h. Solvent was removed in vacuo, and the product isolated using an ion-exchange column of Dowex 50W (H⁺) (10 mL), eluting the amino amide with ammonia (2 M). This gave 4-aminocyclopent-1-enecarboxamide (8, 156 mg, 89% yield). R_f = 0.27 (4:1:1 *n*-butanol/acetic acid/water). ¹H NMR (300 MHz, D₂O): δ 6.32 (1H, s, HC=), 4.03–3.93 (1H, m, CHNH₂), 3.01–2.84 (2H, m, C(3)H, and C(5)H), 2.56–2.43 (2H, m, C(3)H, and C(5)H). ¹³C NMR (300 MHz, D₂O): δ 171.13 (C=O), 140.23 (HC=), 136.08 (=C), 50.91 (CHNH₂), 42.31 (cyclopentene CH₂), 40.52 (cyclopentene CH₂). ESI-MS m/z positive ion mode: 127 (55%, MH⁺), 110 (5%, MH⁺-NH₃); negative ion mode: 126 (20%, M⁻-H).

Site-Directed Mutagenesis. Serine, cysteine, and alanine mutations were generated at the position 102 of ρ_1 subunit by using sense and antisense oligonucleotide primers (Table 1 in the Supporting Information) and the QuickChange II Site-directed Mutagenesis kit protocol (Stratagene, La Jolla, CA). All mutations were verified by DNA sequencing to confirm fidelity (Australian Genome Research Facility, Australia). The plasmids containing wild-type and mutations inserts were linearized with Xba-I, and T7

mMESSAGE mMACHINE kit (Ambion, Austin, TX) was used for mRNA synthesis.

Expression of Wild-Type and Mutant ρ_1 Receptors in *Xenopus* Oocytes. Oocytes from *Xenopus laevis* (South Africa clawed frogs) were harvested as described previously³⁵ in accordance with the National Health and Medical Research Council of Australia's ethical guidelines and approved by the University of Sydney Animal Ethics Committee. Stage V–VI oocytes were injected with 10–15 ng cRNA and then stored at 18 °C in ND 96 solution (96 mM NaCl, 2 mM KCl, 1.8 mM CaCl_2 , 1 mM MgCl_2 , 5 mM HEPES, pH 7.5) supplemented with 2.5 mM sodium pyruvate, 0.5 mM theophylline, 50 $\mu\text{g mL}^{-1}$ gentamycin, and 2.5 mg mL^{-1} tetracycline.

Electrophysiological Recordings. Two to eight days after injections, the activity was measured by two-electrode voltage clamp recording using a Geneclamp 500 amplifier (Axon Instruments, Foster City, CA), a MacLab 2e recorder (AD Instruments, Sydney, NSW, Australia), and Chart version 5.5.6 program as previously described.⁸ Briefly, oocyte expression receptors were clamped at –60 mV with continuous flow of ND96 buffer. Antagonists were screened for inverse agonist activity by applying increasing concentrations (100 and 300 μM) on ρ_1 receptors. SR-95531 (13) and SR-95813 (14) were dissolved in DMSO, and the compounds concentrations were made with the total concentration of 0.8% DMSO. SR-95531 (13) and SR-95813 (14) were not tested higher than 3 mM concentration due to the solubility issues at high concentrations. Antagonist effects were tested in the presence of GABA EC_{50} concentration (20 μM for ρ_{1Y102C} and 200 μM for ρ_{1Y102A} receptors) on ρ_{1Y102C} and ρ_{1Y102A} receptors, and the effects were evaluated for their inhibitory concentration–response actions using ρ_{1Y102C} receptors. For selected antagonists, concentration–inhibition curves were constructed with a minimum of three cells.

Data Analysis. Current responses were normalized to the maximum GABA-activated current recorded in the same cell and expressed as a percentage of this maximum and fitted by least-squares to Hill equation (eq 1). GABA concentration response curves were generated using GraphPad PRISM 5.02 (GraphPad software San Diego, CA).

$$I = I_{\max} [A]^{n_H} / (\text{EC}_{50}^{n_H} + [A]^{n_H}) \quad (1)$$

where I is the current response to a known concentration of agonist, I_{\max} is the maximum current obtained, $[A]$ is the agonist concentration, EC_{50} is the concentration of agonist at which current response is half maximal, and n_H is the Hill coefficient.

Dissociation equilibrium constants (K_B) were determined via the Schild equation (eq 2), where $[B]$ is the antagonist concentration, $[A]$ is the EC_{50} of GABA in the presence of antagonist, and $[A^*]$ is the EC_{50} of GABA in the absence of antagonist. The Schild plot of $\log([A]/[A^*] - 1)$ versus $\log[B]$ was fitted, and the slope was sufficiently close to 1 (see Figure 2 in the Supporting Information). Data are expressed as means \pm standard error of the mean (SEM).

$$K_B = [B] / ([A]/[A^*] - 1) \quad (2)$$

IC_{50} values were calculated using eq 3. The inhibitory concentration curves were generated using GraphPad PRISM 5.02.

$$I = I_{\max} [A]^{n_H} / (\text{IC}_{50}^{n_H} + [A]^{n_H}) \quad (3)$$

I is the peak current at a given concentration of agonist, I_{\max} is the maximal current generated by the concentration of agonist, $[A]$ is the concentration of GABA, IC_{50} is the antagonist concentration, which inhibits 50% of the maximum GABA response, and n_H is the Hill coefficient.

■ ASSOCIATED CONTENT

■ Supporting Information

Information on the oligonucleotide primers, pharmacology of SR-95531 (13), Schild plot analysis, and effect of (\pm)-4-ACPAM (8). This material is available free of charge via the Internet at <http://pubs.acs.org>.

■ AUTHOR INFORMATION

Corresponding Author

*Mailing address: Faculty of Pharmacy, Science Road, Bank building (A15), University of Sydney, NSW, 2006, Australia. Telephone: (+61) 2 9351 8584. Fax (+61) 2 9351 4391. E-mail: mary.collins@sydney.edu.au.

Author Contributions

Participated in research design: I.Y., N.G., K.L., R.D.A., J.E.C., M.C.. Conducted experiments: I.Y., N.G., K.L.. Performed data analysis: I.Y., J.E.C., N.A., M.C.. Wrote or contributed to the writing of the manuscript: I.Y., J.E.C., N.A., N.G., K.L., J.R.H., G.A.R.J., M.C..

Funding

Both I.Y. and N.G. acknowledge the John A. Lamberton Scholarship, and N.G. acknowledges support from an Endeavor International Postgraduate Research Scholarship.

Notes

The authors declare no competing financial interest.

■ ABBREVIATIONS

(+)-4-ACPCA, (+)-4-aminocyclopent-1-ene-1-carboxylic acid; (\pm)-4-ACPAM, (\pm)-4-aminocyclopent-1-enecarboxamide; (\pm)-*cis*-3-ACPBPA, (\pm)-*cis*-(3-aminocyclopentyl)-butylphosphinic acid; (\pm)-*trans*-3-ACPBPA, (\pm)-*trans*-(3-aminocyclopentyl)butylphosphinic acid; (S)-4-ACPBPA, [S]-4-amino-1-cyclopent-1-enyl(butyl)phosphinic acid; 3-APMPA, 3-aminopropyl(methyl)phosphinic acid; 4-GBA, 4-guanidinobutanoic acid; CGP-36742 or SGS-742, (3-aminopropyl-*n*-butylphosphinic acid; DAVA, 5-aminovaleric acid; EC_{50} , effective concentration that activates/or inhibits 50% of the maximum response/or spontaneous current; GABA, γ -aminobutyric acid; HEPES, 4-(2-hydroxyethyl)-1-piperazineethanesulfonic acid; IC_{50} , effective concentration that inhibits 50% of GABA EC_{50} ; LGIC, ligand-gated ion channel; THIP, 4,5,6,7-tetrahydroisoxazolo[5,4-*c*]pyridin-3-ol; TPMPA, (1,2,5,6-Tetrahydropyridin-4-yl)methylphosphinic acid; ZAPA, (Z)-3-[(aminoiminomethyl)thio]prop-2-enoic acid

■ REFERENCES

- (1) Boue-Grabot, E.; Roudbaraki, M.; Bascles, L.; Tramu, G.; Bloch, B., and Garret, M. (1998) Expression of GABA receptor rho subunits in rat brain. *J. Neurochem.* 70, 899–907.
- (2) Rozzo, A.; Armellini, M.; Franzot, J.; Chiaruttini, C.; Nistri, A., and Tongiorgi, E. (2002) Expression and dendritic mRNA localization of GABA_C receptor rho1 and rho2 subunits in developing rat brain and spinal cord. *Eur. J. Neurosci.* 15, 1747–1758.
- (3) Alakuijala, A.; Palgi, M.; Wegelius, K.; Schmidt, M.; Enz, R.; Paulin, L.; Saarma, M., and Pasternack, M. (2005) GABA receptor rho subunit expression in the developing rat brain. *Brain Res. Dev. Brain Res.* 154, 15–23.
- (4) Cunha, C.; Monfils, M. H., and Ledoux, J. E. (2010) GABA_C Receptors in the Lateral Amygdala: A Possible Novel Target for the Treatment of Fear and Anxiety Disorders? *Front. Behav. Neurosci.* 4, 6.
- (5) Stone, R. A.; Liu, J.; Sugimoto, R.; Capehart, C.; Zhu, X., and Pendrak, K. (2003) GABA, experimental myopia, and ocular growth in chick. *Invest. Ophthalmol. Visual Sci.* 44, 3933–3946.
- (6) Arnaud, C.; Gauthier, P., and Gottesmann, C. (2001) Study of a GABA_C receptor antagonist on sleep-waking behavior in rats. *Psychopharmacology (Berlin, Ger.)* 154, 415–419.
- (7) Johnston, G. A. (2002) Medicinal chemistry and molecular pharmacology of GABA(C) receptors. *Curr. Top. Med. Chem.* 2, 903–913.
- (8) Gavande, N.; Yamamoto, I.; Salam, N. K.; Ai, T.-H.; Burden, P. M.; Johnston, G. A. R.; Hanrahan, J. R., and Chebib, M. (2010) Novel

Cyclic Phosphinic Acids as GABA_C ρ Receptor Antagonists: Design, Synthesis, and Pharmacology. *ACS Med. Chem. Lett.* 2, 11–16.

(9) Chebib, M., Hinton, T., Schmid, K. L., Brinkworth, D., Qian, H., Matos, S., Kim, H. L., Abdel-Halim, H., Kumar, R. J., Johnston, G. A., and Hanrahan, J. R. (2009) Novel, potent, and selective GABA_C antagonists inhibit myopia development and facilitate learning and memory. *J. Pharmacol. Exp. Ther.* 328, 448–457.

(10) Ortells, M. O., and Lunt, G. G. (1995) Evolutionary history of the ligand-gated ion-channel superfamily of receptors. *Trends Neurosci.* 18, 121–127.

(11) Enz, R., and Cutting, G. R. (1998) Molecular composition of GABA_C receptors. *Vision Res.* 38, 1431–1441.

(12) Ogurusu, T., Yanagi, K., Watanabe, M., Fukaya, M., and Shingai, R. (1999) Localization of GABA receptor ρ 2 and ρ 3 subunits in rat brain and functional expression of homooligomeric ρ 3 receptors and heterooligomeric ρ 2 ρ 3 receptors. *Recept. Channels* 6, 463–475.

(13) Chebib, M., and Johnston, G. A. (2000) GABA-Activated ligand gated ion channels: medicinal chemistry and molecular biology. *J. Med. Chem.* 43, 1427–1447.

(14) Sedelnikova, A., Smith, C. D., Zakharkin, S. O., Davis, D., Weiss, D. S., and Chang, Y. (2005) Mapping the ρ 1 GABA_C receptor agonist binding pocket. Constructing a complete model. *J. Biol. Chem.* 280, 1535–1542.

(15) Cederholm, J. M., Schofield, P. R., and Lewis, T. M. (2009) Gating mechanisms in Cys-loop receptors. *Eur. Biophys. J.* 39, 37–49.

(16) Hilf, R. J., and Dutzler, R. (2008) X-ray structure of a prokaryotic pentameric ligand-gated ion channel. *Nature* 452, 375–379.

(17) Hilf, R. J., and Dutzler, R. (2009) Structure of a potentially open state of a proton-activated pentameric ligand-gated ion channel. *Nature* 457, 115–118.

(18) Kash, T. L., Trudell, J. R., and Harrison, N. L. (2004) Structural elements involved in activation of the gamma-aminobutyric acid type A (GABA_A) receptor. *Biochem. Soc. Trans.* 32, 540–546.

(19) Wagner, D. A., and Czajkowski, C. (2001) Structure and dynamics of the GABA binding pocket: A narrowing cleft that constricts during activation. *J. Neurosci.* 21, 67–74.

(20) Torres, V. L., and Weiss, D. S. (2002) Identification of a tyrosine in the agonist binding site of the homomeric ρ 1 gamma-aminobutyric acid (GABA) receptor that, when mutated, produces spontaneous opening. *J. Biol. Chem.* 277, 43741–43748.

(21) Lummis, S. C. R., Harrison, N. J., Wang, J., Ashby, J. A., Millen, K. S., Beene, D. L., Dougherty, D. A. (2011) Multiple Tyrosine Residues Contribute to GABA Binding in the GABA_C Receptor Binding Pocket, *ACS Chem. Neurosci.* published online Dec 15, 2011. DOI: 10.1021/cn200103n

(22) Abdel-Halim, H., Hanrahan, J. R., Hibbs, D. E., Johnston, G. A., and Chebib, M. (2008) A molecular basis for agonist and antagonist actions at GABA_C receptors. *Chem. Biol. Drug Des.* 71, 306–327.

(23) Harrison, N. J., and Lummis, S. C. (2006) Locating the carboxylate group of GABA in the homomeric ρ GABA_A receptor ligand-binding pocket. *J. Biol. Chem.* 281, 24455–24461.

(24) Gallagher, M. J., and Cohen, J. B. (1999) Identification of amino acids of the torpedo nicotinic acetylcholine receptor contributing to the binding site for the noncompetitive antagonist [³H]tetracaine. *Mol. Pharmacol.* 56, 300–307.

(25) Zhang, J., Xue, F., and Chang, Y. (2008) Structural determinants for antagonist pharmacology that distinguish the ρ 1 GABA_C receptor from GABA_A receptors. *Mol. Pharmacol.* 74, 941–951.

(26) Holden, J. H., and Czajkowski, C. (2002) Different residues in the GABA_A receptor α 1T60- α 1K70 region mediate GABA and SR-95531 actions. *J. Biol. Chem.* 277, 18785–18792.

(27) Hanrahan, J. R., Mewett, K. N., Chebib, M., Burden, P. M., and Johnston, G. A. R. (2001) An improved, versatile synthesis of the GABA_C antagonists (1,2,5,6-tetrahydropyridin-4-yl)methylphosphinic acid (TPMPA) and (piperidin-4-yl)methylphosphinic acid (P4MPA). *J. Chem. Soc., Perkin Trans. 1*, 2389–2392.

(28) Hanrahan, J. R., Mewett, K. N., Chebib, M., Matos, S., Eliopoulos, C. T., Crean, C., Kumar, R. J., Burden, P., and Johnston, G. A. (2006) Diastereoselective synthesis of (\pm)-(3-aminocyclopentane)-alkylphosphinic acids, conformationally restricted analogues of GABA. *Org. Biomol. Chem.* 4, 2642–2649.

(29) Kumar, R. J., Chebib, M., Hibbs, D. E., Kim, H. L., Johnston, G. A., Salam, N. K., and Hanrahan, J. R. (2008) Novel gamma-aminobutyric acid ρ 1 receptor antagonists; synthesis, pharmacological activity and structure-activity relationships. *J. Med. Chem.* 51, 3825–3840.

(30) Allan, R. D., and Fong, J. (1986) γ -Aminobutyric acid. Synthesis of analogs of GABA. XV. Preparation and resolution of some potent cyclopentene and cyclopentane derivatives. *Aust. J. Chem.* 39, 855–864.

(31) Chebib, M., Gavande, N., Wong, K. Y., Park, A., Premoli, I., Mewett, K. N., Allan, R. D., Duke, R. K., Johnston, G. A., and Hanrahan, J. R. (2009) Guanidino acids act as ρ 1 GABA_C receptor antagonists. *Neurochem. Res.* 34, 1704–1711.

(32) Allan, R. D., Dickenson, H. W., Johnston, G. A. R., Kazlauskas, R., and Mewett, K. N. (1997) Structural analogues of ZAPA as GABA_A agonists. *Neurochem. Int.* 30, 583–591.

(33) Gavande, N., Johnston, G. A., Hanrahan, J. R., and Chebib, M. (2010) Microwave-enhanced synthesis of 2,3,6-trisubstituted pyridazines: application to four-step synthesis of gabazine (SR-95531). *Org. Biomol. Chem.* 8, 4131–4136.

(34) Locock, K. E., Johnston, G. A., and Allan, R. D. (2009) GABA analogues derived from 4-aminocyclopent-1-enecarboxylic acid. *Neurochem. Res.* 34, 1698–1703.

(35) Chebib, M., Mewett, K. N., and Johnston, G. A. (1998) GABA_C receptor antagonists differentiate between human ρ 1 and ρ 2 receptors expressed in *Xenopus* oocytes. *Eur. J. Pharmacol.* 357, 227–234.

(36) Chebib, M., Vandenberg, R. J., Froestl, W., and Johnston, G. A. (1997) Unsaturated phosphinic analogues of gamma-aminobutyric acid as GABA_C receptor antagonists. *Eur. J. Pharmacol.* 329, 223–229.

(37) Ng, C. K., Kim, H. L., Gavande, N., Yamamoto, I., Kumar, R. J., Mewett, K. N., Johnston, G. A., Hanrahan, J. R., and Chebib, M. (2011) Medicinal chemistry of ρ GABA_C receptors. *Future Med. Chem.* 3, 197–209.

(38) Chebib, M., Duke, R. K., Allan, R. D., and Johnston, G. A. (2001) The effects of cyclopentane and cyclopentene analogues of GABA at recombinant GABA_C receptors. *Eur. J. Pharmacol.* 430, 185–192.

(39) Woodward, R. M., Polenzani, L., and Miledi, R. (1993) Characterization of bicuculline/baclofen-insensitive (ρ -like) gamma-aminobutyric acid receptors expressed in *Xenopus* oocytes. II. Pharmacology of gamma-aminobutyric acidA and gamma-aminobutyric acidB receptor agonists and antagonists. *Mol. Pharmacol.* 43, 609–625.